Structural Engineering and Mechanics, *Vol. 75, No. 1 (2020) 59-69*
DOI: https://doi.org/10.12989/sem.2020.75.1.059

Hygrothermoelasticity in a porous cylinder under nonlinear coupling between heat and moisture

Masayuki Ishihara*[1], Taku Yoshida[1], Yoshihiro Ootao[1] and Yoshitaka Kameo[2]

[1]*Graduate School of Engineering, Osaka Prefecture University, 1-1 Gakuen-cho, Naka-ku, Sakai-shi, Osaka 599-8531, Japan*
[2]*Institute for Frontier Life and Medical Sciences, Kyoto University, 53 Kawahara-cho, Shogoin, Sakyo-ku, Kyoto 606-8507, Japan*

(Received March 19, 2019, Revised November 26, 2019, Accepted January 9, 2020)

Abstract. The purpose of this study is to develop practical tools for the mechanical design of cylindrical porous media subjected to a broad gap in a hygrothermal environment. The planar axisymmetrical and transient hygrothermoelastic field in a porous hollow cylinder that is exposed to a broad gap of temperature and dissolved moisture content and is free from mechanical constraint on all surfaces is investigated considering the nonlinear coupling between heat and binary moisture and the diffusive properties of both phases of moisture. The system of hygrothermal governing equations is derived for the cylindrical case and solved to illustrate the distributions of hygrothermal-field quantities and the effect of diffusive properties on the distributions. The distribution of the resulting stress is theoretically analyzed based on the fundamental equations for hygrothermoelasticity. The safety hazard because of the analysis disregarding the nonlinear coupling underestimating the stress is illustrated. By comparing the cylinder with an infinitesimal curvature with the straight strip, the significance to consider the existence of curvature, even if it is infinitesimally small, is demonstrated qualitatively and quantitatively. Moreover, by investigating the bending moment, the necessities to consider an actual finite curvature and to perform the transient analysis are illustrated.

Keywords: diffusion; porous medium; binary moisture; nonlinear coupling; hygrothermal stress; cylinder

1. Introduction

Porous media in engineering applications are usually subjected to a coupled field of heat and moisture and the resulting stresses. For safe design or operation of the applications, the coupled hygrothermoelastic field in media needs to be elucidated. To elucidate the field, the hygrothermal problems and the subsequent elastic problems need to be analyzed. For the former problems, the linear system of governing equations with respect to temperature and moisture content (or vapor concentration) has been employed. In the derivation of that system, two-phase media composed of the substantial solid and voids were considered, the changes in temperature, dissolved moisture content, and vapor concentration were assumed to be linear with each other, and moisture was assumed to be carried through the voids, not through the substantial solid (Hartranft and Sih 1980). For the latter problems, the fundamental equations of elasticity that take into consideration the effects of eigen strains caused by temperature and moisture content have been employed (Sih *et al*. 1986). The thus-analyzed hygrothermal or resulting elastic fields were studied for various cases (Sih *et al*. 1980, Sih and Shih 1980, Sih and Ogawa 1982, Chang *et al*. 1991, Chang 1994, Chang and Weng 1997, Sugano and Chuuman 1993, Dai and Dai 2016, Zhang and Li 2017, Dai *et al*. 2017, 2019a, b).

As in the case of lumber, which is subjected to conditions ranging from dry air to saturated moist air, porous media are often subjected to a broad range of hygrothermal environmental conditions, and moisture can be carried through voids and substantial solids. In such cases, the assumption of linearity among temperature, dissolved moisture content, and vapor concentration and the assumption of the flow only through the voids are no longer valid, and the system of governing equations mentioned above would incorrectly estimate the hygrothermoelastic field. Because of these concerns, the system of governing equations that take into consideration the nonlinear relationship among temperature, dissolved moisture content, and vapor concentration and the diffusivities of both dissolved moisture and vapor was derived (Ishihara *et al*. 2014). Based on that system of equations, the transient-field quantities, such as temperature, moisture content, and stresses, were investigated for an infinite strip subjected to a broad gap of hygrothermal environment, and thereby the nonlinear moisture content distribution at the steady stage and the residual stress at the steady stage, both of which would never be found by the linear hygrothermoelastic theory, were confirmed (Ishihara *et al*. 2016).

The above mentioned investigation (Ishihara *et al*. 2016) was conducted within the framework of a one-dimensional problem in the Cartesian coordinate system to concentrate on investigating the effects of nonlinearity among hygrothermal quantities and binary diffusivity of moisture on the field by eliminating the geometrical complexity. In many engineering applications, however, the problems must be handled in terms of cylindrical coordinates. For example,

*Corresponding author, Associate Professor
E-mail: ishihara@me.osakafu-u.ac.jp

ISSN: 1225-4568 (Print), 1598-6217 (Online)

cylindrical columns of wood are common, material defects—such as cracks, voids, knots, and pith—are often cylindrical, and catalyst carriers of hollow cylinders are often found.

In this study, therefore, on the basis of the above-mentioned nonlinear coupled theory (Ishihara *et al*. 2014), the hygrothermoelastic problem described by a cylindrical coordinate system is treated as a first attempt. The analytical model is an infinite hollow cylinder that is exposed to broad gaps of temperature and dissolved moisture content on inner and outer surfaces and thereby experiences a planar axisymmetrical hygrothermal field, i.e., a one-dimensional hygrothermal field with respect to the radial direction. Also, the model is assumed to be free from mechanical traction and, therefore, in an axisymmetrical plane strain state. The system of hygrothermal governing equations (Ishihara *et al*. 2014) is described for the present case and is solved using the finite-difference method to illustrate numerically the distributions of hygrothermal field quantities, such as temperature, dissolved moisture content, vapor concentration, and dissolution rate. Next, the effect of diffusive properties on the distributions is investigated. Then, the distribution of the resulting stresses is theoretically analyzed, based on the fundamental equations for hygrothermoelasticity. Finally, the effect of the curvature of the cylinder on that stress distribution is investigated.

2. Hygrothermal field in a cylinder considering nonlinear coupling between heat and binary moisture

2.1 Theoretical analysis

The analytical model is an infinite cylinder with inner radius a and outer radius b that occupies the region $\{(r,\theta,z)\,|\,a\le r\le b\}$ in the cylindrical coordinate system (r,θ,z), as shown in Fig. 1. The cylinder is made of a uniform porous medium that consists of voids and substantial solid.

Moisture is assumed to be in the dissolved and gaseous forms in the substantial solid and voids, respectively. The dissolved moisture content M and the vapor concentration C are defined, respectively, as the mass of dissolved moisture per unit mass of the substantial solid and as the mass of gaseous moisture—namely, vapor per unit volume of the voids. In the above-mentioned approach (Ishihara *et al*. 2014), the (absolute) temperature T, dissolved moisture content M, and vapor concentration C are considered to be distributed continuously as functions of the location. This approach defines the mass densities of the dried substantial solid and the porous medium, ρ_s and ρ, respectively, and the volume fraction of the voids f, all of which are also defined in the macroscopic sense satisfying the relationship $\rho=\rho_s(1-f)$. Then, the total mass of moisture per unit mass of the substantial solid, m, is obtained by the sum,

$$\rho m=\rho M+fC. \tag{1}$$

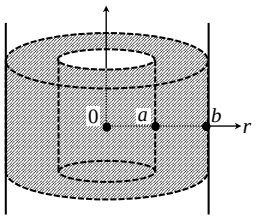

Fig. 1 Analytical model

The dissolved and gaseous moistures are considered, at all times, to be in an equilibrium state that depends on the absolute temperature, which gives the relationship $C=C(M,T)$. The concrete example was presented previously (Ishihara *et al*. 2014), by considering the equilibrium between the dissolved and gaseous moistures, as

$$\left.\begin{aligned}&C(M,T)\\&=f_d(T_0)\frac{p_{st}(T_0)}{R_gT}\exp\left[-\frac{L_{\text{dissolution}}}{R_g}\left(\frac{1}{T}-\frac{1}{T_0}\right)\right]\frac{\omega_sM}{1+\omega_sM}\end{aligned}\right\}, \tag{2}$$

where T_0, $f_d(T)$, $p_{st}(T)$, R_g, $L_{\text{dissolution}}$, and ω_s denote a reference absolute temperature that can be chosen arbitrarily, the *activity coefficient*, the saturated vapor pressure, the gas constant of the moisture, the heat generated by the dissolution of the unit mass of gaseous moisture into the substantial solid, and the constant dependent on the combination of the moisture and substantial solid.

From the above-mentioned macroscopic viewpoint and equilibrium nature, the initial and boundary conditions are described in terms of M and T as functions of location (r,θ,z) and time variable t. In this study, to concentrate on the effects of nonlinear relation, as illustrated by Eq. (2) and the geometric configurations with curvature on the hygrothermoelastic field, the considerably simple conditions are assumed as follows.

$$\left.\begin{aligned}&t=0: T=T_i,\ M=M_i;\\&r=a: T=T_a,\ M=M_a;\\&r=b:\ T=T_b,\ M=M_b\end{aligned}\right\}, \tag{3}$$

where T_i, M_i, T_a, T_b, M_a, and M_b are spatially uniform. In that case, the hygrothermal field is reduced to a planar-axisymmetrical one—in other words, the field is independent of the circumferential and axial coordinates θ and z.

From Fourier's law and Fick's law, the heat flux q_h and the mass flux of the dissolved moisture q_d and gaseous moisture q_g in the radial direction are related to the radial gradients of the field quantities as

$$q_h=-k\frac{\partial T}{\partial r},\ q_d=-D_d\frac{\partial(\rho M)}{\partial r},\ q_g=-D_g\frac{\partial(fC)}{\partial r}. \tag{4}$$

In Eq. (4), k denotes the thermal conductivity, and D_d and D_g denote the diffusivities of the dissolved and gaseous

moistures, respectively, which are referred to as the *dissolved moisture diffusivity* and *gas diffusivity*, respectively, for brevity. These diffusivities are considered isotropic to simplify the problem.

The balance of heat and that of mass are described, respectively, as

$$\left.\begin{aligned} c\rho\frac{\partial T}{\partial t} &= -\left(\frac{\partial}{\partial r}+\frac{1}{r}\right)q_h + \rho L_{\text{dissolution}}\left(\frac{\partial M}{\partial t}\right)_{\text{dissolution}}, \\ \frac{\partial(\rho m)}{\partial t} &= -\left(\frac{\partial}{\partial r}+\frac{1}{r}\right)q_d - \left(\frac{\partial}{\partial r}+\frac{1}{r}\right)q_g \end{aligned}\right\}. \quad (5)$$

In Eq. (5), $-(\partial/\partial r+1/r)q_h$, $-(\partial/\partial r+1/r)q_d$, and $-(\partial/\partial r+1/r)q_g$ denote the influxes of heat, dissolved moisture, and gaseous moisture, respectively. Moreover, c denotes the specific heat, and $(\partial M/\partial t)_{\text{dissolution}}$ denotes the contribution by dissolution for the time rate of dissolved moisture content, which is referred to as the dissolution rate and related to $\partial M/\partial t$ as

$$\rho\frac{\partial M}{\partial t} = -\left(\frac{\partial}{\partial r}+\frac{1}{r}\right)q_d + \rho\left(\frac{\partial M}{\partial t}\right)_{\text{dissolution}}. \quad (6)$$

By substituting Eq. (4) into Eq. (5) combined with Eqs. (1) and (6) and arranging the results, the system of nonlinear coupling diffusion equations is obtained for the present problem as follows.

$$\left.\begin{aligned} &D_T(M,T)\left(\frac{\partial^2}{\partial r^2}+\frac{1}{r}\frac{\partial}{\partial r}\right)T + N_T(M,T) \\ &\quad = \frac{\partial T}{\partial t} - \nu_M(M,T)\frac{\partial M}{\partial t}, \\ &D_M(M,T)\left(\frac{\partial^2}{\partial r^2}+\frac{1}{r}\frac{\partial}{\partial r}\right)M + N_M(M,T) \\ &\quad = \frac{\partial M}{\partial t} + \lambda_T(M,T)\frac{\partial T}{\partial t} \end{aligned}\right\}, \quad (7)$$

where

$$\left.\begin{aligned} D_T(M,T) &= \frac{1}{\Delta_T}\left(\kappa + \frac{D_d D_g}{D_d'}\frac{f\omega}{\rho}\frac{L_{\text{dissolution}}}{c}\right), \\ D_M(M,T) &= \frac{1}{\Delta_M}\left(D_d' + \frac{D_d D_g}{\kappa}\frac{f\omega}{\rho}\frac{L_{\text{dissolution}}}{c}\right), \\ \nu_M(M,T) &= \frac{1}{\Delta_T}\frac{D_g - D_d}{D_d'}\frac{f\sigma}{\rho}\frac{L_{\text{dissolution}}}{c}, \\ \lambda_T(M,T) &= \frac{1}{\Delta_M}\left(1-\frac{D_g}{\kappa}\right)\frac{f\omega}{\rho}, \\ N_T(M,T) &= \frac{1}{\Delta_T}\frac{D_d D_g}{D_d'}\frac{L_{\text{dissolution}}}{c}\frac{f}{\rho}N_{\nabla^2 C}(M,T), \\ N_M(M,T) &= \frac{1}{\Delta_M}D_g\frac{f}{\rho}N_{\nabla^2 C}(M,T), \\ \kappa &= \frac{k}{c\rho}, \quad D_d' = D_d + D_g\frac{f\sigma}{\rho}, \\ \Delta_T &= 1+\frac{D_d}{D_d'}\frac{f\omega}{\rho}\frac{L_{\text{dissolution}}}{c}, \\ \Delta_M &= 1+\frac{f\sigma}{\rho}+\frac{D_g}{\kappa}\frac{f\omega}{\rho}\frac{L_{\text{dissolution}}}{c}, \\ \sigma &= \frac{\partial C}{\partial M}, \ \omega = \frac{\partial C}{\partial T}, \\ \sigma_{,M} &= \frac{\partial\sigma}{\partial M}, \ \sigma_{,T} = \frac{\partial\sigma}{\partial T}, \ \omega_{,M} = \frac{\partial\omega}{\partial M}, \ \omega_{,T} = \frac{\partial\omega}{\partial T}, \\ N_{\nabla^2 C}(M,T) &= \sigma_{,M}\left(\frac{\partial M}{\partial r}\right)^2 + (\sigma_{,T}+\omega_{,M})\frac{\partial T}{\partial r}\frac{\partial M}{\partial r} + \omega_{,T}\left(\frac{\partial T}{\partial r}\right)^2 \end{aligned}\right\}. \quad (8)$$

In deriving Eqs. (7) and (8), all the material properties— ρ_s, ρ, f, $L_{\text{dissolution}}$, k, D_d, D_g, and c —are spatially uniform, as stated in conjunction with Fig. 1, and are assumed to be independent of the field quantities M and T to simplify the problem.

The solution to Eq. (7) subjected to Eq. (3) can be obtained by a finite-difference method. More specifically, the domain $a \le r \le b$ is divided into n_{fdm} equal parts, and Eq. (7) is regarded as the time evolution equation for $2(n_{\text{fdm}}+1)$-degree-of-freedom field quantities, namely, the temperature and dissolved moisture content at thus-generated $(n_{\text{fdm}}+1)$ discrete points. The spatial derivatives required on the left-hand sides of Eq. (7) are evaluated by the corresponding finite differences with truncation errors on the order of the segment length squared. Time evolution is evaluated by the Adams method, in which the predictor–corrector method by the Adams–Bashforth and Adams–Moulton methods is employed (LeVeque 2007).

If the relationship $C = C(M,T)$ is linear, a differential form $\mathrm{d}C = \sigma\mathrm{d}M + \omega\mathrm{d}T$ obtained from Eq. (8) has constant coefficients σ and ω; therefore, the terms $N_T(M,T)$ and $N_M(M,T)$ are absent, as found in Eq. (8). In that case, Eq. (7) for a steady state is reduced to the system of harmonic equations as follows:

$$\left(\frac{\partial^2}{\partial r^2}+\frac{1}{r}\frac{\partial}{\partial r}\right)T = 0, \left(\frac{\partial^2}{\partial r^2}+\frac{1}{r}\frac{\partial}{\partial r}\right)M = 0. \quad (9)$$

The solution to Eq. (9) subjected to the boundary conditions in Eq. (3) can then be obtained in a closed form as

$$T = T_a + (T_b - T_a)\frac{\ln(r/a)}{\ln(b/a)}, \ M = M_a + (M_b - M_a)\frac{\ln(r/a)}{\ln(b/a)}, \quad \text{... (10)}$$

which are harmonic with respect to r. In this respect, the terms $N_T(M,T)$ and $N_M(M,T)$ in Eq. (7), which manifest themselves because of the nonlinearity in $C = C(M,T)$, are the sources that give rise to nonharmonic distributions of M and T in a steady state. The deviation from the harmonic distributions, as found in Eq. (10) due to the nonlinearity in $C = C(M,T)$, is one of the concerns in this study.

2.2 Numerical results

The following nondimensional quantities were introduced to extract the governing parameters:

$$\left.\begin{aligned}
&\hat{T} \equiv \frac{T-T_0}{T_0},\ \hat{C}\left(M,\hat{T}\right) \equiv \frac{fC(M,T)}{\rho},\ \left(\hat{D}_d,\hat{D}_g\right) \equiv \frac{\left(D_d,D_g\right)}{\kappa},\\
&\hat{C}_{st0} \equiv \frac{f}{\rho}\frac{p_{st}(T_0)}{R_gT_0},\ \hat{L}_{\text{dissolution}} \equiv \frac{L_{\text{liquefaction}}}{R_gT_0},\ \hat{c} = \frac{c}{R_g},\\
&\hat{r} \equiv \frac{r}{b},\ \hat{a} \equiv \frac{a}{b},\ \hat{t} \equiv \frac{\kappa t}{b^2},\ \hat{T}_i \equiv \frac{T_i-T_0}{T_0},\\
&\hat{T}_a \equiv \frac{T_a-T_0}{T_0},\ \hat{T}_b \equiv \frac{T_b-T_0}{T_0},\ \hat{M}_{\text{dissolution}} \equiv \frac{b^2}{\kappa}\left(\frac{\partial M}{\partial t}\right)_{\text{dissolution}}
\end{aligned}\right\}. \quad \text{... (11)}$$

The reference absolute temperature is chosen to be $T_0 = 298.15[\mathrm{K}](=25[^\circ\mathrm{C}])$. Sitka spruce (a species of wood) is chosen as the porous medium and water to play the role of moisture. The required parameters are given as $\hat{L}_{\text{dissolution}} = 18.347$, $\hat{C}_{st0} = 35.834\times10^{-6}$, $\omega_s = 3.3333$, $f_d(T_0) \cong 2.1111$, and $\hat{c} = 2.7214$ (Ishihara *et al.* 2016). The value $\hat{D}_d = 10^{-2}$ is chosen unless otherwise stated, because a typical value of the thermal diffusivity for wood is found to be on the order of $10^{-7}\,[\mathrm{m^2/s}]$ (Glass and Zelinka 2010), and a typical value of the dissolved moisture diffusivity for Sitka spruce is found to be on the order of $10^{-9}\,[\mathrm{m^2/s}]$ (Nakao 1998). Because the gas is considered to be more diffusive than dissolved moisture, an example value of $\hat{D}_g = 1$ is chosen unless otherwise stated. The initial and boundary values for the absolute temperature and dissolved moisture content are taken as

$$\left.\begin{aligned}
&T_i = T_0,\ T_a = T_0,\ T_b = 1.2T_0,\\
&M_i = 0.12,\ M_a = 0.12,\ ,\ M_b = 0.2
\end{aligned}\right\}, \quad (12)$$

which are rewritten in non-dimensional forms as

$$\left.\begin{aligned}
&\hat{T}_i = 0,\ \hat{T}_a = 0,\ \hat{T}_b = 0.2,\\
&M_i = 0.12,\ M_a = 0.12,\ ,\ M_b = 0.2
\end{aligned}\right\}. \quad (13)$$

Note that $T_b = 357.78[\mathrm{K}](=84.63[^\circ\mathrm{C}])$ from Eq. (12), the value 0.12 for M_i and M_a is a representative value for the dissolved moisture content under the *air-dried condition* (Bergman 2010), and the value 0.2 for M_b is intended to represent a moderate value compared with the fiber saturation point, namely, approximately 0.3 (Glass and Zelinka 2010). As for the finite-difference method, the division number is taken as $n_{\text{fdm}} = 100$.

Figure 2 shows the variation of vapor concentration with dissolved moisture content and temperature, as illustrated by Eq. (2). If the relationship $C = C(M,T)$ is linear, a differential form $\mathrm{d}C = \sigma\mathrm{d}M + \omega\mathrm{d}T$ obtained from Eq. (8) has constant coefficients σ and ω, as mentioned above, and therefore the curve in Fig. 2 is reduced to a flat plane.

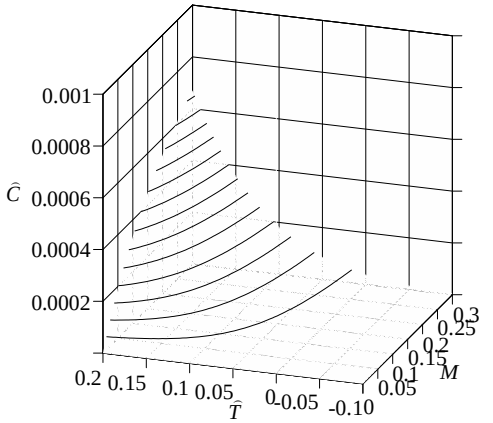

Fig. 2 Variation of vapor concentration with dissolved moisture content and temperature

Figures 3 (a)–(d) show the distributions of the temperature, dissolved moisture content, vapor concentration, and dissolution rate for $\hat{a} = 0.5$. In the following figures, including Figs. 3 (b)–(d), the solid lines indicate the numerical results based on the nonlinear relationship illustrated by Eq. (2), and the dotted lines indicate the numerical results based on the assumption that the relationship $C = C(M,T)$ is linear, with σ and ω in Eq. (8) specified for $M = M_i$ and $T = T_i$. In Fig. 3 (a), only the numerical result based on the nonlinear relationship in $C = C(M,T)$, however, is shown, because the distributions by the linear relationship in $C = C(M,T)$ happen to fall into those by the nonlinear relationship. Figure 3 (b) shows that the dissolved moisture content increases from the humid side, $\hat{r} = 1$, but reaches a steady state at $\hat{t} = 10$, even slower than the temperature does, owing to the difference between the order of the thermal conductivity and that of the dissolved moisture diffusivity $\left(\hat{D}_d = 10^{-2}\right)$. Moreover, in Fig. 3 (b), it is remarkable that the magnitude of dissolved moisture content based on the nonlinear relationship reaches approximately a 9% higher value than that based on the linear relationship, as found for $\hat{t} = 10$ and $\hat{r} = 0.715$. According to this result, it is surmised that the stress derived from the nonlinear relationship in $C = C(M,T)$ also shows higher values than that derived from the linear relationship.

The steady distribution shown in Fig. 3 (c) is found to exhibit positive curvature, i.e., $\partial^2 C/\partial r^2 > 0$, and positive gradient, i.e., $\partial C/\partial r > 0$; therefore, $\partial^2 C/\partial r^2 + 1/r\cdot\partial C/\partial r > 0$ is satisfied. From Eq. (4), the masses of dissolved moisture and vapor flowing into the unit volume of the porous medium per unit time are expressed, respectively, by

$$\left.\begin{aligned}
&-\left(\frac{\partial}{\partial r}+\frac{1}{r}\right)q_d = D_d\rho\left(\frac{\partial^2 M}{\partial r^2}+\frac{1}{r}\frac{\partial M}{\partial r}\right),\\
&-\left(\frac{\partial}{\partial r}+\frac{1}{r}\right)q_g = D_g\rho\left(\frac{\partial^2 C}{\partial r^2}+\frac{1}{r}\frac{\partial C}{\partial r}\right)
\end{aligned}\right\}. \quad (14)$$

Therefore, the profile of $\partial^2 C/\partial r^2 + 1/r \cdot \partial C/\partial r > 0$, shown in Fig. 3 (c), signifies that a local portion of the body is subjected to the inflow of vapor. Meanwhile, because the mass of total moisture flowing into a local portion must be kept zero for the steady state, the relation $(\partial/\partial r + 1/r)q_d = -(\partial/\partial r + 1/r)q_g$ must hold from Eq. (5). From Eq. (14) and $\partial^2 C/\partial r^2 + 1/r \cdot \partial C/\partial r > 0$, this relation leads to $(\partial/\partial r + 1/r)q_d > 0$, which signifies that a local portion of the body is subjected to the outflow of dissolved moisture. Therefore, the dissolved moisture must be supplied by the dissolution of gaseous moisture into the substantial solid. From Eq. (6) and the relation $(\partial/\partial r + 1/r)q_d > 0$ for the steady state, the relation

$$\rho\left(\frac{\partial M}{\partial t}\right)_{\text{dissolution}} = \left(\frac{\partial}{\partial r} + \frac{1}{r}\right)q_d > 0 \tag{15}$$

holds, which is compatible with $(\partial M/\partial t)_{\text{dissolution}} > 0$, shown in Fig. 3 (d). Figure 3 (d) shows that the magnitude of the dissolution rate based on the nonlinear relationship in $C = C(M,T)$ reaches far higher values than those based on the linear relationship.

The structure of the hygrothermal field for the steady state is integrated into Fig. 4. In Fig. 4, the $\hat{r}$ axis lies radially, and the arc lengths of the upper and lower annular sectors appear in a ratio of 0.3 to 0.7, reflecting the volume fraction of voids $f = 0.7$ that was used in a previous work (Ishihara *et al.* 2014) to construct the parameters in Subsection 2.2. Moreover, the depths of blue and red denote the values of M and $\hat{C}$ shown in Figs. 3 (b) and (c), respectively; the radial arrows in the upper and lower annular sectors correspond to the mass flux vectors of dissolved moisture q_d and gaseous moisture q_g, respectively, given by Eq. (4). The lengths of the tangential arrows at the interface of the annular sectors are proportional to the value of $\hat{M}_{\text{dissolution}}$ shown in Fig. 3 (d). Figure 4 shows approximately that the moisture supplied at the humid surface $(\hat{r} = 1)$ diffuses toward the air-dried surface $(\hat{r} = 0.5)$ in the gaseous form at first, transforms into the dissolved form, and diffuses in the dissolved form.

The effect of diffusive properties on the moisture distribution is studied next. At first, $m = M + \hat{C}$ is obtained from Eqs. (1) and (11), which denotes that the total mass of moisture per unit mass of the substantial solid is the sum of the dissolved moisture content and the nondimensional vapor concentration. Meanwhile, by comparing Figs. 3 (b) and (c), M is found to be much greater than $\hat{C}$. Hence, the total mass of moisture can be evaluated substantially by the mass of dissolved moisture. Considering this viewpoint, a measure of the total mass of moisture (per unit axial length of the hollow cylinder) is introduced, and it is defined in a nondimensional form by

$$W = \int_{\hat{a}}^{1} 2\pi \hat{r} M \mathrm{d}\hat{r} \,. \tag{16}$$

The measure W for the linear and steady case given by Eq. (10), denoted by W_{linear}, is calculated as $W_{\text{linear}} = \pi\left[M_b - M_a\hat{a}^2 - (M_b - M_a)(1-\hat{a}^2)/(2\ln\hat{a})\right]$. Therefore, the ratio of the difference $W - W_{\text{linear}}$ to W_{linear}, namely,

$$R_{\text{nonlinear}} = \frac{W - W_{\text{linear}}}{W_{\text{linear}}} \tag{17}$$

can be regarded as one of the measures for the deviation in moisture distribution from the distribution given by Eq. (10). Figure 5 shows the variation of that measure with the dissolved moisture diffusivity $\hat{D}_d$ and gas diffusivity $\hat{D}_g$. Figure 5 shows that the deviation increases with the increase in gas diffusivity and the decrease in dissolved moisture diffusivity. Moreover, the contours in Fig. 5 exhibit a relation $\log_{10}\hat{D}_g \cong \log_{10}\hat{D}_d$ +(constant) i.e., $\hat{D}_g/\hat{D}_d \cong$(constant), which signifies that the magnitude of the deviation is roughly determined by the ratio of the gas diffusivity to the dissolved moisture diffusivity.

3. Transient hygrothermoelastic field

In this section, the resulting stress in the cylinder shown in Fig. 1 that is subjected to the hygrothermal field treated in Section 2 is investigated. The elastic properties are assumed to be isotropic.

3.1 Theoretical analysis

To investigate the stress that occurs only because of the hygrothermal field and excludes the effects of mechanical constraints, the cylinder is considered free from stresses on the inner and outer surfaces and at the infinite ends. As stated in Section 2, the hygrothermal field is planar-axisymmetrical. In that case, the hygrothermoelastic field in the cylinder is considered to be in a generalized plane strain and axisymmetrical state. The governing equations of the field (Sih *et al*. 1986, Noda *et al*. 2003) are the equilibrium equations of stresses

$$\frac{\partial \sigma_{rr}}{\partial r} + \frac{\sigma_{rr} - \sigma_{\theta\theta}}{r} = 0 \,, \tag{18}$$

the strain-displacement equations

$$\varepsilon_{rr} = \frac{\partial u_r}{\partial r}, \; \varepsilon_{\theta\theta} = \frac{u_r}{r} \,, \tag{19}$$

and the generalized Hooke's law

$$\left.\begin{aligned}
\varepsilon_{rr} &= \frac{1-\nu^2}{E}\left(\sigma_{rr} - \frac{\nu}{1-\nu}\sigma_{\theta\theta}\right) \\
&\quad + (1+\nu)\alpha\Delta T + (1+\nu)\beta\Delta M - \nu\varepsilon_0, \\
\varepsilon_{\theta\theta} &= \frac{1-\nu^2}{E}\left(\sigma_{\theta\theta} - \frac{\nu}{1-\nu}\sigma_{rr}\right) \\
&\quad + (1+\nu)\alpha\Delta T + (1+\nu)\beta\Delta M - \nu\varepsilon_0, \\
\varepsilon_0 &= \frac{1}{E}\left[\sigma_{zz} - \nu(\sigma_{rr} + \sigma_{\theta\theta})\right] + \alpha\Delta T + \beta\Delta M
\end{aligned}\right\}, \tag{20}$$

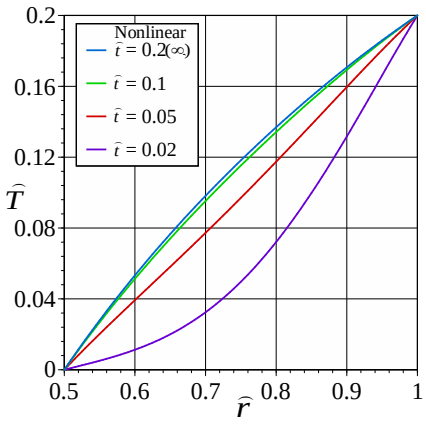

(a) Temperature

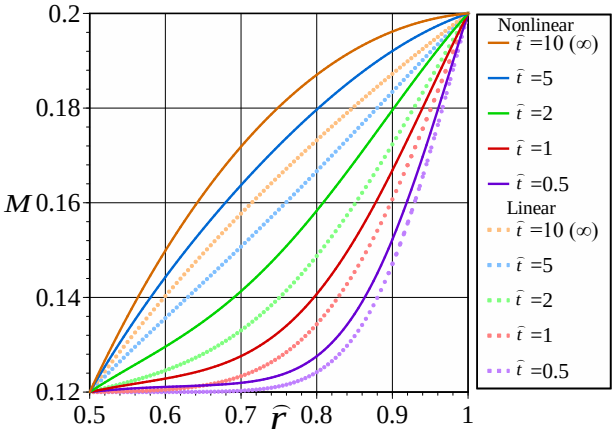

(b) Dissolved moisture content

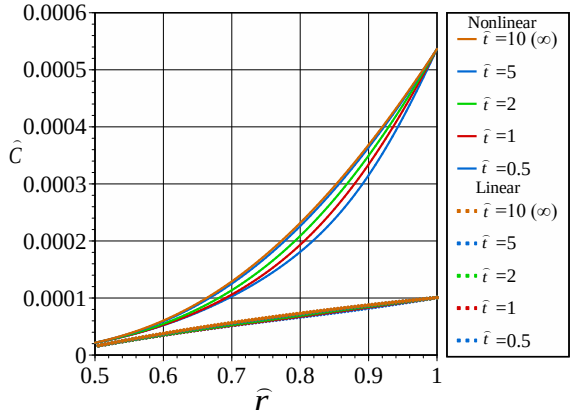

(c) Vapor concentration

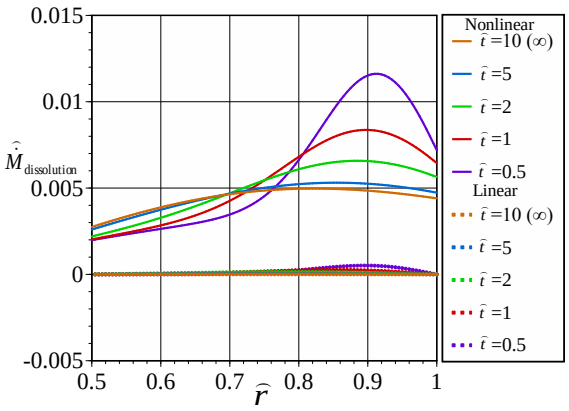

(d) Dissolution rate

Fig. 3 Distributions of hygrothermal quantities $(\hat{a}=0.5)$

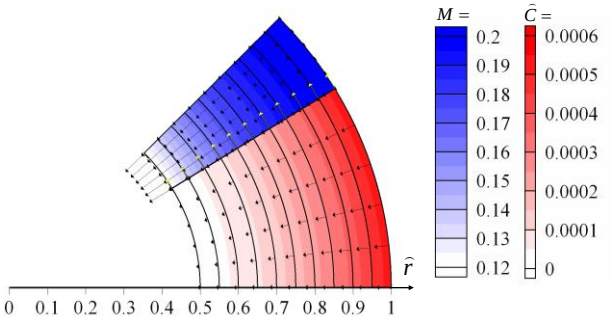

Fig. 4 Structure of hygrothermal field for steady state $(\hat{t}=10;\ \hat{a}=0.5)$

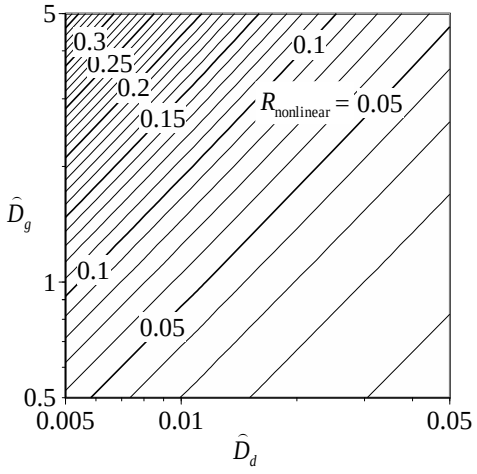

Fig. 5 Effects of diffusive properties on deviation $(\hat{t}\to\infty;\ \hat{a}=0.5)$

where σ_{rr}, $\sigma_{\theta\theta}$, and σ_{zz} denote the radial, hoop, and axial stresses, respectively; ε_{rr} and $\varepsilon_{\theta\theta}$ denote the radial and hoop strains, respectively; u_r denotses the radial displacement; E and ν denote the Young's modulus and Poisson's ratio, respectively; α and β denote the coefficients of thermal and moisture expansion, respectively; ε_0 denotes the axial strain that occurs because of the unconstraint at the infinite ends;

$$\Delta T \equiv T - T_{\text{free}},\ \Delta M \equiv M - M_{\text{free}}; \tag{21}$$

and T_{free} and M_{free} denote the absolute temperature and dissolved moisture content, respectively, that give a natural state, i.e., $\varepsilon_{ij}=0$ and $\sigma_{ij}=0$.

By substituting Eq. (19) into Eq. (20), solving that result with respect to the stresses, and then substituting the stresses into Eq. (18), Navier's equation is obtained as

$$\frac{\partial}{\partial r}\left[\frac{1}{r}\frac{\partial(ru_r)}{\partial r}\right]=\frac{1+\nu}{1-\nu}(\alpha\Delta T+\beta\Delta M). \tag{22}$$

The general solutions of the displacement, strains and stresses are obtained by integrating Eq. (22) successively, and substituting that result into Eqs. (19) and (20). The integral constants involved are determined by the boundary conditions

$$r=a,\, b:\sigma_{rr}=0, \tag{23}$$

the axial strain ε_0 is determined by the unconstraint condition at the infinite ends

$$\int_a^b \sigma_{zz}\cdot 2\pi r\mathrm{d}r=0, \tag{24}$$

and thereby the solutions of the field quantities are obtained finally as

$$\left.\begin{aligned}
u_r&=\frac{1+\nu}{1-\nu}\left[\begin{aligned}&\frac{1}{r}\int_a^r(\alpha\Delta T+\beta\Delta M)r\mathrm{d}r\\&+\left(\frac{1-3\nu}{1+\nu}r+\frac{a^2}{r}\right)\\&\times\frac{1}{b^2-a^2}\int_a^b(\alpha\Delta T+\beta\Delta M)r\mathrm{d}r\end{aligned}\right],\\
\sigma_{rr}&=\frac{E}{1-\nu}\left[\begin{aligned}&-\frac{1}{r^2}\int_a^r(\alpha\Delta T+\beta\Delta M)r\mathrm{d}r\\&+\frac{r^2-a^2}{r^2(b^2-a^2)}\int_a^b(\alpha\Delta T+\beta\Delta M)r\mathrm{d}r\end{aligned}\right],\\
\sigma_{\theta\theta}&=\frac{E}{1-\nu}\left[\begin{aligned}&\frac{1}{r^2}\int_a^r(\alpha\Delta T+\beta\Delta M)r\mathrm{d}r\\&+\frac{r^2+a^2}{r^2(b^2-a^2)}\int_a^b(\alpha\Delta T+\beta\Delta M)r\mathrm{d}r\\&-(\alpha\Delta T+\beta\Delta M)\end{aligned}\right],\\
\sigma_{zz}&=\frac{E}{1-\nu}\left[\frac{2}{b^2-a^2}\int_a^b(\alpha\Delta T+\beta\Delta M)r\mathrm{d}r-(\alpha\Delta T+\beta\Delta M)\right]
\end{aligned}\right\}. \tag{25}$$

If the relationship $C=C(M,T)$ is linear, the temperature and dissolved moisture content for a steady state is obtained as Eq. (10). In that case, by substituting Eq. (10) into Eq. (25), the in-plane stresses, i.e., the radial and hoop stresses for a steady state, are reduced to

$$\left.\begin{aligned}
\sigma_{rr}&=[\alpha(T_b-T_a)+\beta(M_b-M_a)]\\
&\quad\cdot\frac{E}{2(1-\nu)}\left[-\frac{\ln(r/a)}{\ln(b/a)}+\left(1-\frac{a^2}{r^2}\right)\frac{b^2}{b^2-a^2}\right],\\
\sigma_{\theta\theta}&=[\alpha(T_b-T_a)+\beta(M_b-M_a)]\\
&\quad\cdot\frac{E}{2(1-\nu)}\left[-\frac{1+\ln(r/a)}{\ln(b/a)}+\left(1+\frac{a^2}{r^2}\right)\frac{b^2}{b^2-a^2}\right]
\end{aligned}\right\}. \tag{26}$$

Because the nonlinearity in $C=C(M,T)$ gives rise to the deviation in hygrothermal distributions from those in Eq. (10), as mentioned above, it gives rise to the deviation also in the resulting stress distributions from those in Eq. (26). The consequences resulting from the deviation, more specifically, the undesirable stresses adverse to safe design or operation of the related applications, are the primary concerns here and are discussed in the following subsection.

In addition, the consequences of the model's having curvature are also concerns. The infinite strip, as shown in Fig. 6, that was subjected to the conditions given by Eq. (3) with $r=a,\, b$ replaced with $x=0,\, L$ and was free from mechanical constraint on the surfaces $x=0,\, L$ and at the infinite ends was previously treated (Ishihara *et al*. 2016).

To compare the cylinder shown in Fig. 1 with the strip shown in Fig. 6, the relations

$$L\equiv b-a,\; x\equiv r-a,\; \hat{L}\equiv\frac{L}{b} \tag{27}$$

are applied to the cylinder shown in Fig. 1. The quantity $1/b$ represents the curvature of the cylinder, and, therefore, the parameter $\hat{L}$ denotes the nondimensional curvature with reference to the thickness L. Then, the temperature, dissolved moisture content, and stresses given by Eqs. (10) and (25) are rewritten as

$$\left.\begin{aligned}
T&=T_a+(T_b-T_a)\frac{\ln\left[1-\left(1-\frac{x}{L}\right)\hat{L}\right]-\ln(1-\hat{L})}{-\ln(1-\hat{L})},\\
M&=M_a+(M_b-M_a)\frac{\ln\left[1-\left(1-\frac{x}{L}\right)\hat{L}\right]-\ln(1-\hat{L})}{-\ln(1-\hat{L})},\\
\sigma_{rr}&=[\alpha(T_b-T_a)+\beta(M_b-M_a)]\\
&\quad\cdot\frac{E}{2(1-\nu)}\left\{\begin{aligned}&-\frac{\ln\left[1-\left(1-\frac{x}{L}\right)\hat{L}\right]-\ln(1-\hat{L})}{-\ln(1-\hat{L})}\\&+\frac{\left[1-\left(1-\frac{x}{L}\right)\hat{L}\right]^2-(1-\hat{L})^2}{\left[1-\left(1-\frac{x}{L}\right)\hat{L}\right]^2\left[1-(1-\hat{L})^2\right]}\end{aligned}\right\},\\
\sigma_{\theta\theta}&=[\alpha(T_b-T_a)+\beta(M_b-M_a)]\\
&\quad\cdot\frac{E}{2(1-\nu)}\left\{\begin{aligned}&-\frac{1+\ln\left[1-\left(1-\frac{x}{L}\right)\hat{L}\right]-\ln(1-\hat{L})}{-\ln(1-\hat{L})}\\&+\frac{\left[1-\left(1-\frac{x}{L}\right)\hat{L}\right]^2+(1-\hat{L})^2}{\left[1-\left(1-\frac{x}{L}\right)\hat{L}\right]^2\left[1-(1-\hat{L})^2\right]}\end{aligned}\right\}
\end{aligned}\right\}. \tag{28}$$

When the outer radius b tends to sufficiently larger compared with the thickness L in the cylinder, i.e.,

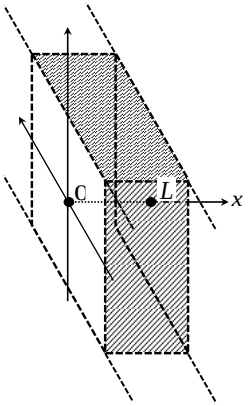

Fig. 6 Infinite strip

$\hat{L}\to 0$, the hygrothermoelastic circumstances in the cylinder is supposedly regarded as approaching those in the infinite strip shown in Fig. 6. When $\hat{L}\to 0$, the expressions in Eq. (28) are reduced to

$$\left.\begin{aligned} &T=T_a+\left(T_b-T_a\right)\frac{x}{L},\ M=M_a+\left(M_b-M_a\right)\frac{x}{L},\\ &\sigma_{rr}=0,\\ &\sigma_{\theta\theta}=\left[\alpha\left(T_b-T_a\right)+\beta\left(M_b-M_a\right)\right]\frac{E}{2(1-\nu)}\left(1-2\cdot\frac{x}{L}\right)\end{aligned}\right\}. \quad (29)$$

Thus-obtained linear distributions in T and M and null distribution in the stress in the thickness direction σ_{rr}, all of which are for a steady state under the linear relation in $C=C(M,T)$, are similar to those obtained for the strip shown in Fig. 6 (Ishihara *et al*. 2016). However, the in-plane stress $\sigma_{\theta\theta}$ given by Eq. (29) exhibits a significant distribution, which is linear with respect to the thickness direction, whereas the in-plane stress in the strip exhibited a null distribution (Ishihara *et al*. 2016). Thus, even for the limited case of the steady field under the linear relation in $C=C(M,T)$, the field in the cylinder with an infinitesimal curvature $\hat{L}\to 0$ is qualitatively different from the field in the strip, unlike the supposition that both circumstances are similar to each other.

The numerical results presented in the following subsection include the effects of various factors. Specifically, with reference to the strip in the steady field under the linear relation in $C=C(M,T)$, the sequential effects of the nonlinearity in $C=C(M,T)$, the model's having infinitesimal curvature $\hat{L}\to 0$, the finiteness of curvature, and the transient nature of the field participate in the results in the following subsection.

3.2 Numerical results

In this subsection, the distributions of hygrothermoelastic stresses given by Eq. (25) are numerically illustrated. In addition to Eq. (11), the nondimensional quantities are introduced as

$$\left.\begin{aligned} &\left(\hat{\sigma}_{rr},\hat{\sigma}_{\theta\theta}\right)=\frac{1-\nu}{\alpha E T_0}\left(\sigma_{rr},\sigma_{\theta\theta}\right),\ \hat{u}_r=\frac{1-\nu}{\alpha T_0 b}u_r,\\ &\hat{\beta}=\frac{\beta}{\alpha T_0},\ \hat{T}_{\text{free}}=\frac{T_{\text{free}}-T_0}{T_0}\end{aligned}\right\}. \quad (30)$$

By applying Eqs. (11) and (30) to Eq. (25) with Eq. (21) substituted, the nondimensional in-plane stresses are formulated as

$$\left.\begin{aligned} \hat{u}_r&=(1+\nu)\left[\begin{aligned}&\frac{1}{\hat{r}}\int_{\hat{a}}^{\hat{r}}\left(\Delta\hat{T}+\hat{\beta}\Delta M\right)\hat{r}\,\mathrm{d}\hat{r}\\ &+\left(\frac{1-3\nu}{1+\nu}\hat{r}+\frac{\hat{a}^2}{\hat{r}}\right)\frac{1}{1-\hat{a}^2}\int_{\hat{a}}^{1}\left(\Delta\hat{T}+\hat{\beta}\Delta M\right)\hat{r}\,\mathrm{d}\hat{r}\end{aligned}\right],\\ \hat{\sigma}_{rr}&=\left[\begin{aligned}&-\frac{1}{\hat{r}^2}\int_{\hat{a}}^{\hat{r}}\left(\Delta\hat{T}+\hat{\beta}\Delta M\right)\hat{r}\,\mathrm{d}\hat{r}\\ &+\frac{\hat{r}^2-\hat{a}^2}{\hat{r}^2\left(1-\hat{a}^2\right)}\int_{\hat{a}}^{1}\left(\Delta\hat{T}+\hat{\beta}\Delta M\right)\hat{r}\,\mathrm{d}\hat{r}\end{aligned}\right],\\ \hat{\sigma}_{\theta\theta}&=\left[\begin{aligned}&\frac{1}{\hat{r}^2}\int_{\hat{a}}^{\hat{r}}\left(\Delta\hat{T}+\hat{\beta}\Delta M\right)\hat{r}\,\mathrm{d}\hat{r}\\ &+\frac{\hat{r}^2+\hat{a}^2}{\hat{r}^2\left(1-\hat{a}^2\right)}\int_{\hat{a}}^{1}\left(\Delta\hat{T}+\hat{\beta}\Delta M\right)\hat{r}\,\mathrm{d}\hat{r}-\left(\Delta\hat{T}+\hat{\beta}\Delta M\right)\end{aligned}\right]\end{aligned}\right\}, \quad \text{... (31)}$$

where $\Delta\hat{T}\equiv\hat{T}-\hat{T}_{\text{free}}$. As derived in previous work (Ishihara *et al*. 2016), the nondimensional coefficient of moisture expansion is given as

$$\hat{\beta}=24.572. \quad (32)$$

Equations (31) and (32) show that the effect of moisture expansion on the stress is considerably predominant over that of thermal expansion, for unit changes in nondimensional temperature and dissolved moisture content. The absolute temperature and dissolved moisture content for a natural state are chosen as $T_{\text{free}}=T_i$ and $M_{\text{free}}=M_i$, respectively.

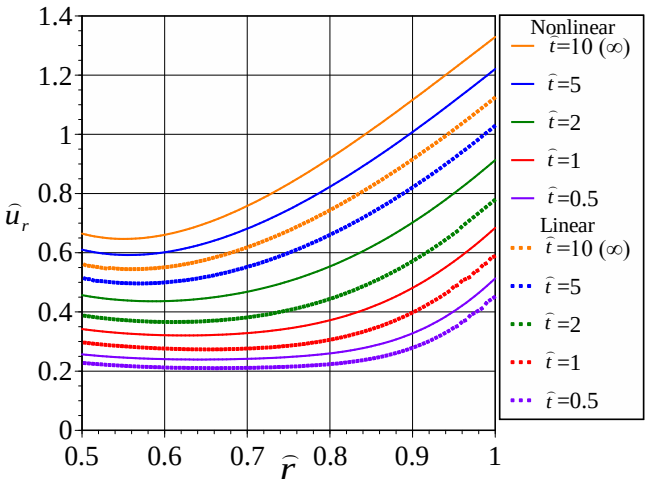

(a) Radial displacement $(\nu=1/3)$

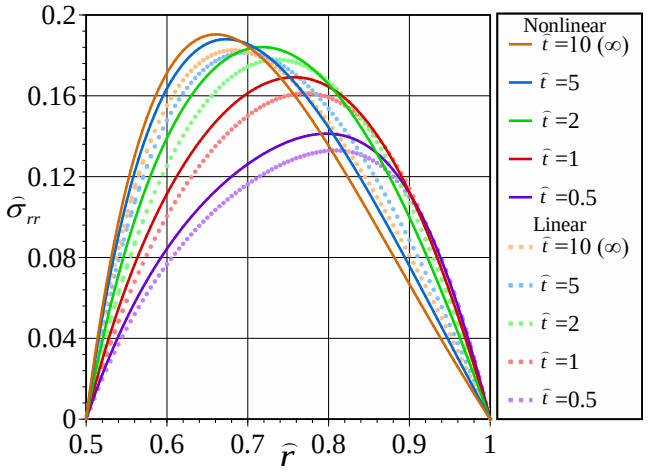

(b) Radial stress

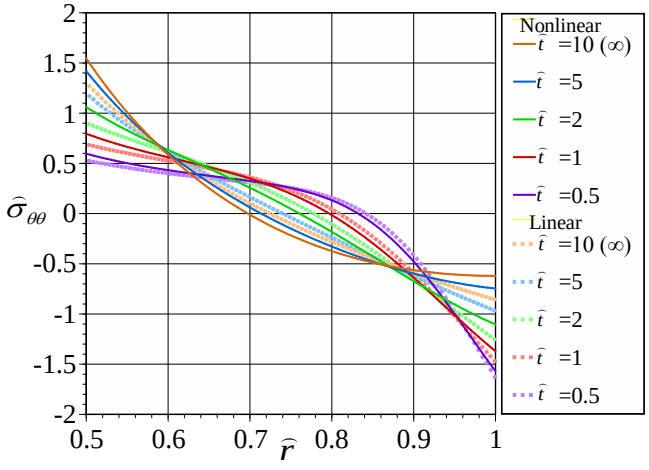

(c) Tangential stress

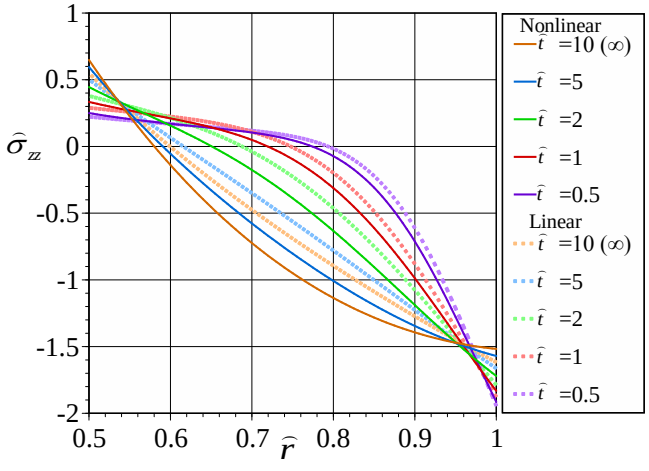

(d) Axial stress

Fig. 7 Distributions of hygrothermoelastic field quantities in cylinder $(\hat{a} = 0.5)$

At first, the effect of the nonlinear relation in $C = C(M,T)$ on the hygrothermoelastic field is investigated. Figure 7 shows the distributions of the hygrothermoelastic field quantities in the cylinder. Because of the predominant effect of the aforementioned moisture expansion, the distributions at the same stages as in Fig. 3 (b) are chosen in Fig. 7. The qualitative and quantitative difference in the field is found in Fig. 7. For instance, Figures 3 (b) and 7 (b) show that the peaks in the distributions of radial stress shift toward the dry surface as the dissolved moisture diffuses toward that surface. Moreover, the magnitudes of the maximum radial stress based on the nonlinear relation in $C = C(M,T)$ are found to be greater than those based on the linear relation (up to approximately a 6% higher value at $\hat{t} = 0.5$). This result indicates that the investigation based on the linear relation in $C = C(M,T)$ underestimates the risk of failure. Similar underestimation is also found in the tangential and axial stresses at the inner surface as found in Figs. 7 (c) and (d). It should be noted that these hazards can never be found by the linear assumption in $C = C(M,T)$ as performed in previous studies (Sih *et al*. 1980, Sih and Shih 1980, Sih and Ogawa 1982, Chang *et al*. 1991, Chang 1994, Chang and Weng 1997, Sugano and Chuuman 1993, Dai and Dai 2016, Zhang and Li 2017, Dai *et al*. 2017, 2019a, b). Therefore, it is significant to consider the nonlinear relation in $C = C(M,T)$ when investigating the hygrothermoelastic stress in terms of safe design and operation of the related applications.

Then, to investigate the effect of the model's having infinitesimal curvature $\hat{L} \to 0$, attention is paid to the tangential stress, because that stress is significantly affected by that effect, as mentioned in the previous subsection. To perform numerical calculations, a certain curvature $\hat{L} = 0.001$ is regarded as an infinitesimal curvature $\hat{L} \to 0$. Figure 8 shows the distributions of the tangential stress in the cylinder based on the nonlinear relation in $C = C(M,T)$ for a steady state and its counterpart in the strip, i.e., the in-plane stress $\hat{\sigma}$. The in-plane stress based on the linear relation in $C = C(M,T)$ vanishes, as described in previous work (Ishihara *et al*. 2016). Figure 8 shows that the tangential stress in the cylinder exhibits a significant distribution compared with the in-plane stress in the strip. Therefore, it is significant to consider the existence of curvature, even if the curvature is infinitesimally small, when investigating the hygrothermoelastic stress in terms of safe design and operation of the related applications. The difference of the stress distributions in the cylinder and the strip is explained by considering the tangential force and bending moment (per unit axial length) defined, respectively, by

$$N = \int_0^L \sigma_{\theta\theta} \cdot \mathrm{d}x,\ K = \int_0^L \sigma_{\theta\theta} \cdot \left(x - \frac{L}{2} \right) \mathrm{d}x\,. \tag{33}$$

By considering the axisymmetricity of field and the equilibrium of forces in the free body sectioned as, for example, $\{(r,\theta,z) \mid a \le r \le b,\ 0 \le \theta \le \pi\}$ or by inspecting Fig. 8, the tangential force in the cylinder is found to be absent as found in the strip (Ishihara *et al*. 2016). However, by inspecting Fig. 8, the bending moment in the cylinder is

found to be present $\left(K/\left[L^2\cdot\alpha ET_0/(1-\nu)\right]\cong 0.187\right)$ unlike the strip (Ishihara *et al*. 2016). That bending moment and, consequently, the distribution of tangential stress occurs, because the bending deformation is restrained in the cylinder with the infinitesimal curvature.

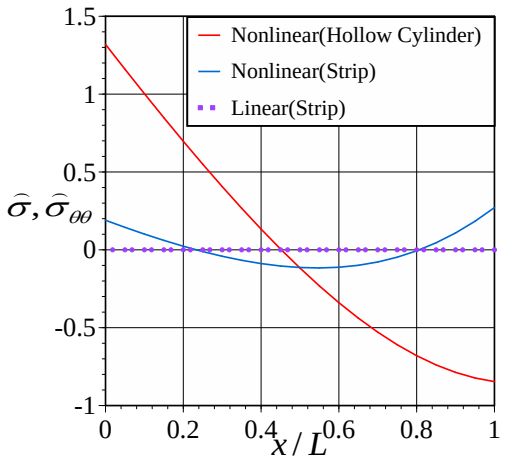

Fig. 8 Distributions of tangential stress in cylinder and in-plane stress in strip $\left(\hat{L}=0.001\right)$

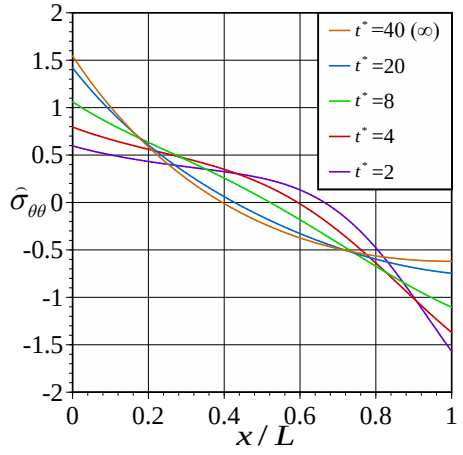

(a) $\hat{L}=0.5$

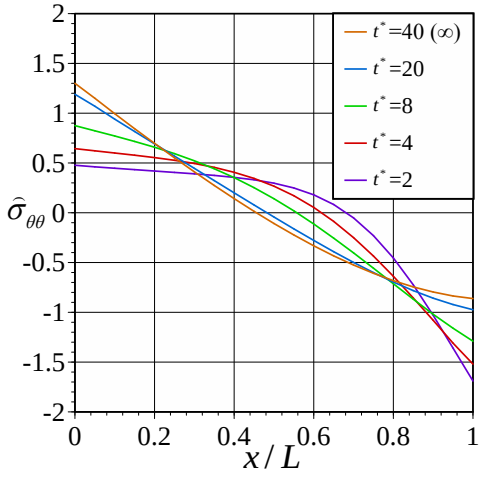

(b) $\hat{L}=0.001$

Fig. 9 Distributions of tangential stress in cylinder

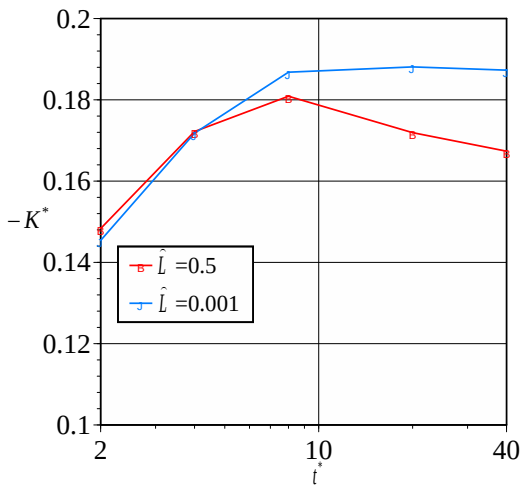

Fig. 10 Variations of bending moment with time

Finally, the effect of the finiteness of curvature is investigated. In Fig. 8, the infinitesimal curvature $\hat{L}\to 0$ was assumed. A cylinder, however, has a finite curvature in general. Therefore, it is necessary to investigate the cylinder with a finite curvature. The certain curvature $\hat{L}=0.5$ is chosen as an example. Figures 9 (a) and (b) show the distributions of the tangential stress in the cylinder with a finite and an infinitesimal curvature, respectively, in which the nondimensional time variable here is defined with reference to the thickness as $t^*\equiv\kappa t/L^2$. From Figs. 9 (a) and (b), both of the distributions appear similar. To investigate their difference quantitatively, the bending moment defined by Eq. (33) is evaluated. Figure 10 shows the variations of the (negative) bending moment with time, in which the nondimensional moment here is defined with reference to the thickness as $K^*\equiv K/\left[L^2\cdot\alpha ET_0/(1-\nu)\right]$. Figure 10 shows that the bending moment in the cylinder with the finite curvature is greater than that with the infinitesimal curvature in a certain early stage. This finding demonstrates the necessity to consider a concrete value of curvature when evaluating the hygrothermoelastic field in cylinders. Moreover, the maximum bending moment in the cylinder with a finite curvature occurs before the field reaches a steady state, which demonstrates the necessity of the transient analysis as performed in this study.

4. Concluding remarks

Based on the nonlinear coupling between heat and binary moisture, a first attempt was made to address the hygrothermoelastic problem described by a cylindrical coordinate system. The analytical model was an infinite hollow cylinder exposed to a broad gap of hygrothermal environment and free from mechanical constraint. The system of hygrothermal governing equations that was derived for the Cartesian coordinate system was extended to describe the present case and was solved using the finite-difference method in order to numerically illustrate the distributions of hygrothermal field quantities, such as

temperature, dissolved moisture content, vapor concentration, and dissolution rate and the effect of diffusive properties on the distributions. Then, the distribution of the resulting stresses was theoretically analyzed based on the fundamental equations for hygrothermoelasticity. As a result, the hazard that the analysis disregarding the nonlinear coupling underestimates the stress was illustrated. Then, by comparing the cylinder with an infinitesimal curvature with the infinite strip, the significance of considering the existence of curvature, even if it is infinitesimally small, was illustrated qualitatively and quantitatively. Moreover, by investigating the bending moment, the necessities to consider an actual curvature and to perform the transient analysis were illustrated.

References

Bergman, R. (2010), "Drying and control of moisture content and dimensional changes", General Technical Report FPL-GTR-190; Forest Products Laboratory, United States Department of Agriculture Forest Service, Madison, WI, USA.

Chang, W.J. (1994), "Transient hygrothermal responses in a solid cylinder by linear theory of coupled heat and moisture", *Appl. Math. Modelling*, **18**(8), 467-473. https://doi.org/10.1016/0307-904X(94)90309-3.

Chang, W.J., Chen, T.C. and Weng, C.I. (1991), "Transient hygrothermal stresses in an infinitely long annular cylinder: coupling of heat and moisture", *J. Therm. Stresses*, **14**(4), 439-454. https://doi.org/10.1080/01495739108927078.

Chang, W.J. and Weng, C.I. (1997), "An analytical solution of a transient hygrothermal problem in an axisymmetric double-layer annular cylinder by linear theory of coupled heat and moisture", *Appl. Math. Modelling*, **21**(11), 721-734. https://doi.org/10.1016/S0307-904X(97)00100-5.

Dai, T. and Dai, H.L. (2016), "Hygrothermal behavior of a CFRR-metal adhesively bonded joint with coupled transfer of heat and moisture through the thickness", *Compos. Struct.*, **152**, 947-958. https://doi.org/10.1016/j.compstruct.2016.05.097.

Dai, T., Yang, Y., Dai, H.L. and Hu, Z.(2019a), "Interfacial stress analysis of a CFRR-metal adhesively bonded joint with/without defect under hygrothermal environment", *Appl. Math. Modelling*, **67**, 357-377. https://doi.org/10.1016/j.apm.2018.10.032.

Dai, T., Yang, Y., Dai, H.L., Tang, H. and Lin, Z.Y. (2019b), "Hygrothermal mechanical behaviors of a porous FG-CRC annular plate with variable thickness considering aggregation of CNTs", *Compos. Struct.*, **215**,198-213. https://doi.org/10.1016/j.compstruct.2019.02.061

Dai, H.-L., Zheng, Z.Q. and Dai, T. (2017), "Investigation on a rotating FGPM circular disk under a coupled hygrothermal field", *Appl. Math. Model.*, **46**, 28-47. https://doi.org/10.1016/j.apm.2017.01.062.

Glass, S.V. and Zelinka, S.L. (2010), "Moisture relations and physical properties of wood", General Technical Report FPL-GTR-190); Forest Products Laboratory, United States Department of Agriculture Forest Service, Madison, WI, USA.

Hartranft, R.J. and Sih, G.C. (1980), "The influence of the Soret and Dufour effects on the diffusion of heat and moisture in solids", *J. Eng. Sci.*, **18**(12), 1375-1383. https://doi.org/10.1016/0020-7225(80)90094-4.

Ishihara, M., Ootao, Y. and Kameo, Y. (2014), "Hygrothermal field considering nonlinear coupling between heat and binary moisture diffusion in porous media", *J. Therm. Stresses*, **37**(10), 1173-1200. https://doi.org/10.1080/01495739.2014.936232.

Ishihara, M., Ogasawara, K., Ootao, Y. and Kameo, Y. (2016), "One-dimensional transient hygrothermoelastic field in a porous strip considering nonlinear coupling between heat and binary moisture", *J. Therm. Sci. Technol.*, **11**(3), 16-00375. https://doi.org/10.1299/jtst.2016jtst0035.

LeVeque, R.J. (2007), *Finite Difference Methods for Ordinary and Partial Differential Equations: Steady-State and Time-Dependent Problems*, Society for Industrial and Applied Mathematics, Philadelphia, PA.

Nakao, T. (1998), "Description of moisture dependence of diffusion coefficient by moisture diffusion equation considering Coulomb friction", *Holz als Roh und Werkstoff*, **56**(4), 266.

Noda, N., Hetnarski, R.B. and Tanigawa, Y. (2003), *Thermal Stresses (2nd ed)*, Taylor & Francis, New York, USA.

Sih, G.C., Michopoulos, J.G. and Chou, S.C. (1986), *Hygrothermoelasticity*, Martinus Nijhoff Publishers, Dordrecht, Netherlands.

Sih, G.C. and Ogawa, A. (1982), "Transient thermal change on a solid surface: coupled diffusion of heat and moisture", *J. Therm. Stresses*, **5**(3-4), 265-282. https://doi.org/10.1080/01495738208942150.

Sih, G.C. and Shih, M.T. (1980), "Hygrothermal stress in a plate subjected to antisymmteric time-dependent moisture and temperature boundary conditions", *J. Therm. Stresses*, **3**(3), 321-340. https://doi.org/10.1080/01495738008926972.

Sih, G.C., Shih, M.T. and Chou, S.C. (1980), "Transient hygrothermal stresses in composites: coupling of moisture and heat with temperature varying diffusivity", *J. Eng. Sci.*, **18**(1), 19-42. https://doi.org/10.1016/0020-7225(80)90004-X.

Sugano, Y. and Chuuman, Y. (1993), "Analytical solution of transient hygrothermoelastic problem due to coupled heat and moisture diffusion in a hollow cylinder", *Transactions of the Japan Soc. Mech. Eng. Series A*, **59**(564), 1956-1963 (in Japanese).

Zhang, X.-Y. and Li, X.-F. (2017), "Transient response of a hygrothermoelastic cylinder based on fractional diffusion wave theory", *J. Therm. Stresses*, **40**(12), 1575-1594. https://doi.org/10.1080/01495739.2017.1344111.

PL